

Neutrophil Extracellular Trap–Derived Enzymes Oxidize High-Density Lipoprotein

An Additional Proatherogenic Mechanism in Systemic Lupus Erythematosus

Carolyne K. Smith,¹ Anuradha Vivekanandan-Giri,² Chongren Tang,³ Jason S. Knight,² Anna Mathew,² Robin L. Padilla,² Brenda W. Gillespie,² Carmelo Carmona-Rivera,¹ Xiaodan Liu,² Venkataraman Subramanian,⁴ Sarfaraz Hasni,¹ Paul R. Thompson,⁴ Jay W. Heinecke,³ Rajiv Saran,² Subramaniam Pennathur,² and Mariana J. Kaplan¹

Objective. Oxidative stress and oxidized high-density lipoprotein (HDL) are implicated as risk factors for cardiovascular disease (CVD) in systemic lupus erythematosus (SLE). Yet, how HDL is oxidized and rendered dysfunctional in SLE remains unclear. Neutrophil extracellular traps (NETs), the levels of which

are elevated in lupus, possess oxidant-generating enzymes, including myeloperoxidase (MPO), NADPH oxidase (NOX), and nitric oxide synthase (NOS). We hypothesized that NETs mediate HDL oxidation, impairing cholesterol efflux capacity (CEC).

Methods. Plasma MPO levels and CEC activity were examined in controls and lupus patients, and 3-chlorotyrosine (MPO specific) and 3-nitrotyrosine (derived from reactive nitrogen species) were quantified in human HDL. Multivariable linear models were used to estimate and test differences between groups. HDL was exposed to NETs from control and lupus neutrophils in the presence or absence of MPO, NOX, NOS inhibitors, and chloroquine (CQ). Murine HDL oxidation was quantified after NET inhibition *in vivo*.

Results. SLE patients displayed higher MPO levels and diminished CEC compared to controls. SLE HDL had higher 3-nitrotyrosine and 3-chlorotyrosine content than control HDL, with site-specific oxidation signatures on apolipoprotein A-I. Experiments with human and murine NETs confirmed that chlorination was mediated by MPO and NOX, and nitration by NOS and NOX. Mice with lupus treated with the NET inhibitor Cl-amidine displayed significantly decreased HDL oxidation. CQ inhibited NET formation *in vitro*.

Conclusion. Active NOS, NOX, and MPO within NETs significantly modify HDL, rendering the lipoprotein proatherogenic. Since NET formation is enhanced in SLE, these findings support a novel role for NET-derived lipoprotein oxidation in SLE-associated CVD and identify additional proatherogenic roles of neutrophils and putative protective roles of antimalarials in autoimmunity.

Supported by the Lupus Research Institute (grant to Dr. Kaplan), the Intramural Research Program of the National Institute of Arthritis and Musculoskeletal and Skin Diseases, and the NIH through Public Health Service grants GM-079357 (to Dr. Thompson), DK-089503 and DK-097153 (to Dr. Pennathur), and HL-088419 (to Dr. Kaplan). Ms Smith's work was supported by Public Health Service grant AI-007413. Dr. Knight is recipient of a Scientist Development Award from the Rheumatology Research Foundation. Dr. Pennathur is recipient of a Within Our Reach grant from the Rheumatology Research Foundation.

¹Carolyne K. Smith, BS, Carmelo Carmona-Rivera, PhD, Sarfaraz Hasni, MD, Mariana J. Kaplan, MD: National Institute of Arthritis and Musculoskeletal and Skin Diseases, NIH, Bethesda, Maryland; ²Anuradha Vivekanandan-Giri, PhD, Jason S. Knight, MD, PhD, Anna Mathew, MBBS, Robin L. Padilla, MS, Brenda W. Gillespie, PhD, Xiaodan Liu, MD, Rajiv Saran, MD, MS, Subramaniam Pennathur, MD: University of Michigan, Ann Arbor; ³Chongren Tang, PhD, Jay W. Heinecke, MD: University of Washington, Seattle; ⁴Venkataraman Subramanian, PhD, Paul R. Thompson, PhD: The Scripps Research Institute, Jupiter, Florida.

Ms Smith and Dr. Vivekanandan-Giri contributed equally to this work. Drs. Pennathur and Kaplan contributed equally to this work.

Dr. Thompson holds the patent for Cl-amidine and is a co-founder of Padlock Therapeutics.

Address correspondence to Subramaniam Pennathur, MD, Department of Internal Medicine, University of Michigan Medical School, 5309 Brehm Center, 1000 Wall Street, Ann Arbor, MI 48105 (e-mail: spennath@umich.edu); or to Mariana J. Kaplan, MD, Systemic Autoimmunity Branch, Intramural Research Program, National Institute of Arthritis and Musculoskeletal and Skin Diseases, NIH, Building 10, 6D47C, 10 Center Drive, MSC 1560, Bethesda, MD 20892 (e-mail: mariana.kaplan@nih.gov).

Submitted for publication December 3, 2013; accepted in revised form May 8, 2014.

Patients with systemic lupus erythematosus (SLE) exhibit enhanced morbidity and mortality from premature atherosclerotic cardiovascular disease (CVD), which is not explained by the Framingham risk equation (1–3). While immune dysregulation plays a prominent role in CVD in SLE, the mechanisms remain unclear. We proposed that altered innate immune responses play important roles in the development of endothelial damage and plaque formation in SLE (4–7). In addition, lipoprotein abnormalities triggered by oxidative stress may promote atherogenesis in systemic autoimmune diseases (3,8–10).

Myeloperoxidase (MPO) is a major source of reactive oxidants within the human vasculature. Classically thought of as macrophage-derived, MPO localizes to atherosclerotic plaques, and its activity is linked to plaque rupture (10–12) and oxidation of high-density lipoprotein (HDL) (8,13,14). In its native form, HDL has vasoprotective properties due to its ability to remove excess cholesterol from arterial wall macrophages, via ATP-binding cassette transporter A1 (ABCA1) interactions, and pleiotropic antiinflammatory and antioxidant effects (10,15–17). When apolipoprotein A-I (Apo A-I), the most abundant protein within HDL, becomes oxidized via chlorination or nitration of tyrosine residues (Cl-Tyr- and N-Tyr-oxidized HDL, respectively), the lipoprotein loses vasoprotective capabilities and gains proinflammatory activity (8,10,13,14,17,18). Patients with chronic inflammatory diseases, including SLE and rheumatoid arthritis (RA), have increased levels of oxidized HDL (8,9). However, the mechanisms and dominant cellular sources leading to HDL oxidation are still unclear.

Phagocytes possess the machinery to oxidize biomolecules and represent attractive candidates for HDL oxidation. In addition to MPO, phagocytes display NADPH oxidase (NOX) activity (19), which can lead to superoxide anion ($O_2^{\bullet-}$) and hydrogen peroxide (H_2O_2) production, both of which are damaging oxidative species. Indeed, increased NOX activity is significantly associated with CVD (19). MPO can transform NOX-generated H_2O_2 into hypochlorous acid (HOCl) if chloride is present, or generate nitrogen dioxide radical (NO_2^{\bullet}), a reactive nitrogen species (RNS), if nitrite is present, promoting both vascular damage and HDL oxidation. Previous studies indicated associations between plasma MPO levels and CVD in the general population, although it remains unclear if this is more relevant to specific patient subsets (11,20). As enhanced circulating MPO activity has been described in SLE (21), this raises the possibility that circulating sources of MPO

play key roles in lipoprotein oxidation in lupus, as previously observed in RA by our group (8).

The 3 isoforms of nitric oxide synthase (NOS) in humans, endothelial cell NOS (eNOS), neuronal NOS (nNOS), and inducible NOS (iNOS), can generate nitric oxide (NO^{\bullet}). While NO^{\bullet} is generally vasoprotective, it can combine with NOX-generated $O_2^{\bullet-}$ to produce the RNS peroxynitrite ($ONOO^-$) or be dismutated into H_2O_2 , leading to HOCl or NO_2^{\bullet} , which are potential oxidizers of HDL. While reports in the literature are mixed (22,23), iNOS is the isoform most associated with CVD risk.

The oxidation of HDL, by NOS/NOX-produced $ONOO^-$ or MPO/NOX-generated NO_2^{\bullet} and HOCl, transforms the lipoprotein into a proatherogenic form that can increase vascular damage and inflammatory cytokine production (10,12,14,15,17,18). While the roles of NOS, NOX, and MPO in CVD are largely associated with macrophages and endothelial cells, these enzymes are important for neutrophil respiratory bursts (12,24,25).

Neutrophil extracellular traps (NETs) are extracellular fibers composed of DNA, histones, and microbicidal granular proteins that play important roles in antimicrobial responses (26,27). NET formation is triggered by microbes, platelets, cytokines, and immune complexes, and is enhanced in various autoimmune disorders including SLE (4,6,26–32). While NET formation pathways are not fully characterized, the process appears to be dependent on MPO, NOX, and peptidyl-arginine deiminase type 4 (PAD4) activity (26,27,32–34). Beyond their role in innate defense mechanisms and autoimmunity, NETs have been implicated in CVD by promoting thrombosis and proatherogenic innate immune responses (1,6,35–37). Neutrophils and NETs have been detected in the vasculature tunica externa and in the lumen (35,38,39). Pertinent to SLE, we identified a subset of aberrant neutrophils in lupus peripheral blood named low-density granulocytes (LDGs), which are primed to form NETs with enhanced oxidant externalization (4,7). We hypothesized that NETs formed by lupus LDGs may represent a prominent source of extracellular NOS, NOX, and MPO, leading to proatherogenic HDL oxidation.

PATIENTS AND METHODS

Patients. Plasma samples were collected from SLE patients who fulfilled the American College of Rheumatology SLE classification criteria (40). Healthy controls were recruited by advertisement. The study was approved by the

University of Michigan and NIH Institutional Review Boards. Lupus disease activity was quantified by the SLE Disease Activity Index (SLEDAI) (41). Pregnant or lactating women and individuals with recent or current infections or liver dysfunction were excluded.

Mice. NZM2328 (NZM) breeding pairs were a gift from Dr. Chaim Jacob (University of Southern California, Los Angeles) (5). BALB/c mice were purchased from The Jackson Laboratory. Mice were bred and housed in a specific pathogen-free barrier facility at the University of Michigan. Female mice were killed at 24 weeks of age, before overt development of renal disease. The protocol was approved by the University of Michigan's Committee on Use and Care of Animals.

Plasma HDL isolation. HDL was isolated from human and murine plasma by sequential ultracentrifugation (8). The protein concentration was estimated with Coomassie staining (Thermo Scientific). Samples were stored at -80°C until analyzed.

Quantification of oxidized amino acids in plasma, HDL, and Apo A-I peptides. Plasma proteins were precipitated and delipidated (8); oxidized amino acids were quantified using isotopically labeled internal standards, $^{13}\text{C}_6$ tyrosine, $^{13}\text{C}_6$ 3-chlorotyrosine, and $^{13}\text{C}_6$ 3-nitrotyrosine, by liquid chromatography-electrospray ionization tandem mass spectrometry (LC-ESI-MS/MS) with multiple reaction monitoring MS/MS positive-ion acquisition mode (42).

Multiple reaction monitoring analysis of oxidized tyrosine-containing Apo A-I peptides with LC-ESI-MS/MS. Plasma HDL samples were delipidated and reduced with dithiothreitol (5 μM ; Sigma-Aldrich) before alkylation with iodoacetamide (15 mM ; Sigma-Aldrich) (8). Samples were trypsin-digested and purified using solid-phase extraction C18 Sep-Pak columns (Waters). Isotopically labeled oxidized (nitrated and chlorinated) peptides and native Apo A-I peptides were spiked into samples following trypsin digestion. Multiple reaction monitoring analysis was performed with an Agilent 6490 Triple Quadrupole MS system equipped with an Agilent 1200 Infinity UPLC (Agilent) in positive ion mode (8).

Cholesterol efflux capacity (CEC) and MPO quantification. CEC assay and MPO quantification were performed as previously described (8). J774 cells were maintained in Dulbecco's modified Eagle's medium (DMEM)/10% fetal bovine serum (FBS; Life Technologies) (43). To radiolabel the cellular free cholesterol pool, cells were incubated with 1 $\mu\text{Ci}/\text{ml}$ ^3H -cholesterol (PerkinElmer) in DMEM/1 mg/ml fatty acid-free bovine serum albumin (BSA) and 5 $\mu\text{g}/\text{ml}$ Acyl-CoA: cholesterol acyltransferase inhibitor Sandoz 58-035 (Sigma-Aldrich) overnight. Cells were incubated with 0.5 mM 8-Br-cAMP for 20 hours to induce ABCA1 expression, incubated with DMEM/fatty acid-free BSA with or without 2.8% Apo B-depleted plasma for 4 hours at 37°C , and then chilled on ice. Medium was collected and filtered, the ^3H -cholesterol content of medium and cells was quantified, and the fraction of total ^3H -cholesterol released into the medium was calculated (8).

Induction and purification of NETs and coculture assays. Human control neutrophils and lupus LDGs were purified from the peripheral blood (4), and murine neutrophils were purified from the bone marrow (6). Cells were plated at a density of 0.25×10^6 cells/ cm^2 on tissue culture plates in RPMI 1640 without phenol red (Life Technologies) for Cl-Tyr quantification, or in Krebs-Ringer phosphate glucose (KRPg;

Sigma-Aldrich) for N-Tyr quantification (4). Neutrophils were cultured in the presence or absence of 20 nM phorbol myristate acetate (PMA; Sigma-Aldrich) for 3 hours (human), or 100 nM PMA for 5 hours (mouse) to induce NET formation (27). Since LDGs form NETs spontaneously, they were left unstimulated. To inhibit NET formation, 200 μM Cl-amidine was added for the full incubation (6). Since NOX and MPO are required for NET formation but are also targets for the conditions in which oxidation was inhibited, cells were allowed to form NETs for 1 hour before adding the following inhibitors: diphenyleiiodonium (DPI), which blocks NOX activity (100 μM ; Tocris), L- N^G -monomethyl-L-arginine (L-NMMA), which blocks NOS activity (200 μM ; Abcam), and 3-amino-1,2,4-triazole (3-AT), which blocks MPO activity (10 mM ; Sigma-Aldrich) (26,27,32,33,44,45). Inhibitors were replenished hourly during NET formation. NETs were isolated as previously described, using 100 units/ml DNase I (Roche) (31). Supernatants resulting from the final spin contained NET-bound proteins and DNA fragments. Control, nonoxidized HDL (50 $\mu\text{g}/\text{ml}$) was incubated with NETs in the presence or absence of L-NMMA, 3-AT, and DPI, for 30 minutes at 37°C . The relative abundance of HDL oxidation was calculated as the fold change of each condition relative to HDL oxidation with NET formation.

Quantification of NOS and NOX in human and murine NETs. Immunoblot analysis. To detect NOS and NOX externalization during NET formation, digested human and murine NETs and whole neutrophil pellets were harvested. NET proteins were precipitated with acetone; 50 μg of NET or whole cell pellet proteins were separated on a 10% sodium dodecyl sulfate-polyacrylamide gel electrophoresis gel. Proteins were transferred onto a nitrocellulose membrane, incubated in 5% BSA/Tris buffered saline/0.1% Tween 20 for 1 hour, and stained with goat anti-mouse p47 or p22 (1:200; Santa Cruz Biotechnology), rabbit anti-eNOS or anti-iNOS (1:100; Abcam), or anti-tubulin (negative control; 1:500) (Sigma-Aldrich), followed by horseradish peroxidase-conjugated rabbit anti-goat (1:1,000; Millipore) or goat anti-rabbit (1:5,000; Jackson ImmunoResearch) secondary antibodies. Densitometry was performed with Quantity One (Bio-Rad).

Fluorescence microscopy. Human control neutrophils and lupus LDGs and mouse neutrophils were seeded onto poly-L-lysine-coated coverslips (Sigma-Aldrich) (4,6), stimulated with PMA as described above, or left unstimulated (for LDGs) before fixing in 4% paraformaldehyde and staining with goat anti-p47 or anti-p22 (both 1:50 dilution; Santa Cruz), or rabbit anti-iNOS or anti-eNOS (both 1:20 dilution; Abcam) for 1 hour at 4°C , followed by staining with secondary fluorochrome-conjugated antibodies (Jackson ImmunoResearch) and Hoechst 33342 (Life Technologies). Coverslips were mounted with ProLong Gold Antifade (Life Technologies). Images were acquired on a Zeiss LSM 510 META laser scanning confocal microscope (Carl Zeiss Microimaging) with a $\times 63$ lens and quantified (4,6).

Effect of chloroquine (CQ) on neutrophils. Whole blood was incubated with 250 ng/ml CQ (Sigma-Aldrich) for 2 hours before neutrophils and LDGs were purified (17). The effect of CQ on NET formation was quantified using a Sytox assay (Life Technologies) (31), immunofluorescence staining, and immunoblotting. To determine the effect of CQ on MPO, NOS, and NOX activity, 1×10^6 granulocytes/ml, in either RPMI 1640 or KRPg with protease inhibitor cocktail (Roche),

were homogenized at 35,000 revolutions per minute (Omni International) for three 10-second intervals on ice before treatment with or without 20 nM PMA for 30 minutes, then in the absence or presence of 250 ng/ml CQ for 30 minutes, and finally with or without 50 μ g/ml HDL for 30 minutes. Samples were frozen and analyzed for Cl-Tyr and N-Tyr oxidation.

In vivo Cl-amidine administration. PAD inhibitor Cl-amidine was synthesized (46). Twelve-week-old female NZM mice were administered daily subcutaneous injections of Cl-amidine (10 mg/kg/day) or phosphate buffered saline (Life Technologies) for 14 weeks (6). Plasma was isolated, and HDL was purified (5).

Statistical analysis. Pearson's correlation coefficients were calculated for the outcomes studied and patient characteristics. Multivariable linear models were used to explore significant predictors of the outcomes of interest. The method of best subsets with the R-squared selection criterion guided the model selection process (8). These models were also used to estimate and test differences between control and SLE groups. Skewed variables were logarithm base 10 or natural log transformed to satisfy statistical assumptions. Normally distributed variables were not transformed. *P* values less than 0.05 were considered significant. Analyses were conducted using SAS V.9.2 or GraphPad Prism version 5.

RESULTS

Patient characteristics. Controls and lupus patients did not differ in demographic characteristics (Table 1). Levels of low-density lipoprotein (LDL) were significantly lower in patients with SLE, possibly associated with prevalent use of statins (22.5%). In SLE patients, use of statins correlated with elevated plasma Cl-Tyr levels, whereas antimalarial use was associated with increased plasma N-Tyr content (Table 2). SLE patients displayed significantly higher levels of plasma MPO than controls (median 425.5 versus 326.7 fmoles/ml; *P* < 0.05). Elevated MPO levels significantly correlated with an increased erythrocyte sedimentation rate and low LDL levels. Oxidation levels did not correlate with SLEDAI scores (Table 2).

Impaired CEC in SLE. The ability of HDL to promote cholesterol efflux from macrophages is a metric of HDL function and has a strong inverse association with CVD (3,14,17). Plasma from patients with SLE displayed significantly diminished CEC when compared to control plasma (mean \pm SD 9.2 \pm 1.6% in controls versus 7.8 \pm 1.5% in SLE patients; *P* = 0.001) (Table 1). These results persisted after adjustment for significant predictors of CEC (Table 2) and support previous indications that dysfunctional HDL present in SLE leads to impaired CEC and may promote proatherogenic responses (3).

Increased chlorinated and nitrated HDL in SLE. Impaired CEC has been associated with HDL modifications such as nitration and chlorination (14,18). We

Table 1. Demographic and clinical characteristics of the healthy controls and SLE patients*

	Healthy controls (n = 20)	Patients with SLE (n = 40)
Age, mean \pm SD years	47.5 \pm 10.9	48.2 \pm 13.5
Sex, no. (%) male	2 (10)	4 (10)
Body mass index, kg/m ²	24.0 (6.6)	27.8 (12.2)
Cholesterol, mg/dl	212.0 (58.0)	150.0 (87.0)
Triglycerides, mg/dl	161.5 (89.0)	124.5 (99.0)
HDL, mg/dl	57.5 (28.0)	52.0 (18.5)
LDL, mean \pm SD mg/dl	128.1 \pm 29.7	92.9 \pm 39.6†
ESR, mm/hour	NA	13.0 (13.0)
C-reactive protein, mg/liter	NA	0.6 (0.7)
SLEDAI	0	3.0 (6.0)†
Treatment, no. (%)		
Steroids	0 (0)	17 (42.5)†
Antimalarials	0 (0)	29 (72.5)†
Statins	0 (0)	9 (22.5)†
Beta-blockers	0 (0)	10 (25)†
ACE inhibitors	0 (0)	9 (22.5)†
MPO, fmoles/ml	326.7 (156.0)	425.5 (212.0)†
Cholesterol efflux capacity, mean \pm SD %	9.2 \pm 1.6	7.8 \pm 1.5†

* Except where indicated otherwise, values are the median (interquartile range). SLE = systemic lupus erythematosus; HDL = high-density lipoprotein; LDL = low-density lipoprotein; ESR = erythrocyte sedimentation rate; NA = not available; SLEDAI = SLE Disease Activity Index; ACE = angiotensin-converting enzyme; MPO = myeloperoxidase.

† *P* < 0.05 versus healthy controls.

quantified levels of Cl-Tyr, a highly specific product of MPO, and N-Tyr, a product of MPO and other RNS-producing enzymes, in HDL isolated from SLE patients and controls and in total plasma (8,42). SLE HDL displayed 1.9-fold higher median levels of N-Tyr (72.3 versus 38.7 μ moles/mole Tyr; *P* = 0.0057) and 120.9-fold higher median levels of Cl-Tyr (229.8 versus 1.9 μ moles/mole Tyr; *P* < 0.0001), compared to control HDL (Figure 1B) even after adjustment (Table 2). Because a majority (72.5%) of the SLE patients were receiving antimalarials (Table 1), we determined the effect of antimalarial treatment in the study population. Adjusting for antimalarial use had no significant effect on the values in Table 1 or Table 2 (data not shown). Since previous studies demonstrated that chlorination of tyrosine residue 192 (Tyr¹⁹²) within the Apo A-I protein most directly associates with impaired CEC (14), with 6 other Apo A-I tyrosine residues (Tyr¹⁸, Tyr²⁹, Tyr¹⁰⁰, Tyr¹¹⁵, Tyr¹⁶⁶, and Tyr²³⁶) as other potential sites of oxidation (8,13), we determined if regiospecific nitration and chlorination patterns occur in SLE. The highest levels of MPO-dependent Cl-Tyr HDL oxidation in SLE samples were observed at tyrosines 192, 115, and 18 (Figure 1C), when compared to control samples. Levels of N-Tyr HDL oxidation were highest at tyrosines 192,

Table 2. Correlations of lipoprotein characteristics and plasma oxidation with clinical features in all subjects and in patients with SLE only*

	MPO†	CEC	HDL Cl-Tyr†	HDL N-Tyr†	Plasma Cl-Tyr†	Plasma N-Tyr
Pearson correlations among all patients (n = 60)						
Age, years						
r	-0.23	0.11	0.03	0.07	-0.05	-0.02
P	0.08	0.39	0.83	0.61	0.71	0.89
Sex, male						
r	-0.21	0.05	0.21	0.14	0.08	0.04
P	0.11	0.72	0.12	0.30	0.54	0.77
BMI, kg/m ² †						
r	0.20	-0.23	0.31‡	0.05	0.18	0.07
P	0.13	0.08	0.02‡	0.72	0.18	0.61
Cholesterol, mg/dl†						
r	-0.13	0.14	-0.04	0.58‡	-0.25	0.23
P	0.33	0.31	0.77	<0.01‡	0.07	<0.10
Triglycerides, mg/dl†						
r	0.11	-0.07	-0.14	0.01	-0.02	-0.16
P	0.44	0.62	0.32	0.94	0.90	0.26
HDL, mg/dl†						
r	-0.25	0.28‡	-0.15	0.04	-0.17	0.01
P	0.08	<0.05‡	0.28	0.79	0.22	0.96
LDL, mg/dl						
r	-0.44‡	0.18	-0.29‡	0.12	-0.46‡	-0.27
P	<0.01‡	0.22	0.04‡	0.41	<0.01‡	0.06
Pearson correlations among SLE patients only (n = 40)						
CRP, mg/liter†						
r	0.05	0.18	0.17	0.11	0.24	-0.16
P	0.76	0.27	0.31	0.52	0.15	0.34
ESR, mm/hour†						
r	0.36‡	0.06	-0.05	0.19	0.07	-0.14
P	0.02‡	0.71	0.75	0.26	0.66	0.40
SLEDAI						
r	0.14	0.08	0.15	0.06	0.15	0.05
P	0.39	0.63	0.34	0.71	0.36	0.76
Steroid use						
r	-0.09	0.11	-0.20	-0.27	0.11	0.09
P	0.59	0.51	0.22	0.09	0.49	0.57
Antimalarial use						
r	0.03	0.08	-0.08	0.05	-0.20	0.32‡
P	0.83	0.64	0.62	0.76	0.23	<0.05‡
Statin use						
r	-0.18	0.13	-0.002	-0.01	0.32‡	-0.12
P	0.26	0.42	0.99	0.95	<0.05‡	0.48
Beta-blocker use						
r	-0.07	0.22	-0.15	-0.26	0.16	-0.004
P	0.66	0.17	0.36	0.11	0.32	0.98
ACE inhibitor use						
r	-0.06	0.16	0.09	0.12	0.01	-0.06
P	0.70	0.33	0.59	0.46	0.96	0.71
Comparisons of MPO, CEC, and lipoprotein profiles between controls and SLE patients§						
Unadjusted comparison						
Controls	5.7 ± 0.1	9.2 ± 0.3	1.4 ± 0.4	2.5 ± 0.4	0.4 ± 0.3	3.4 ± 0.2
SLE patients	6.0 ± 0.1	7.8 ± 0.2	5.4 ± 0.3	4.2 ± 0.3	3.3 ± 0.2	5.7 ± 0.1
P	0.0005	0.0022	<0.0001	0.0003	<0.0001	<0.0001
Model R ²	0.19	0.15	0.51	0.2	0.49	0.64
Adjusted comparison						
Controls	5.8 ± 0.1	9.2 ± 0.3	1.5 ± 0.4	2.6 ± 0.3	0.3 ± 0.3	3.3 ± 0.2
SLE patients	6.0 ± 0.1	8.0 ± 0.3	5.4 ± 0.3	4.1 ± 0.2	3.3 ± 0.2	5.7 ± 0.2
P	0.0198	0.0073	<0.0001	0.0002	<0.0001	<0.0001
Model R ²	0.4	0.21	0.56	0.49	0.62	0.63

* SLE = systemic lupus erythematosus; CRP = C-reactive protein, ESR = erythrocyte sedimentation rate, SLEDAI = SLE Disease Activity Index; ACE = angiotensin-converting enzyme.

† Natural log transformed prior to correlation calculation.

‡ Significant results ($P < 0.05$).

§ Values are the differences in the estimated means between groups ± SEM. Cholesterol efflux capacity (CEC; %) was adjusted for high-density lipoprotein (HDL) ($R^2 = 0.08$; $n = 50$), myeloperoxidase (MPO; fmoles/ml) was adjusted for age, body mass index (BMI), and low-density lipoprotein (LDL) ($r^2 = 0.33$; $n = 49$), HDL 3-chlorotyrosine (Cl-Tyr) was adjusted for BMI ($R^2 = 0.10$; $n = 59$), HDL 3-nitrotyrosine (N-Tyr) was adjusted for cholesterol ($R^2 = 0.34$; $n = 54$), plasma Cl-Tyr was adjusted for LDL ($R^2 = 0.21$; $n = 50$), and plasma N-Tyr was adjusted for LDL ($R^2 = 0.07$; $n = 50$).

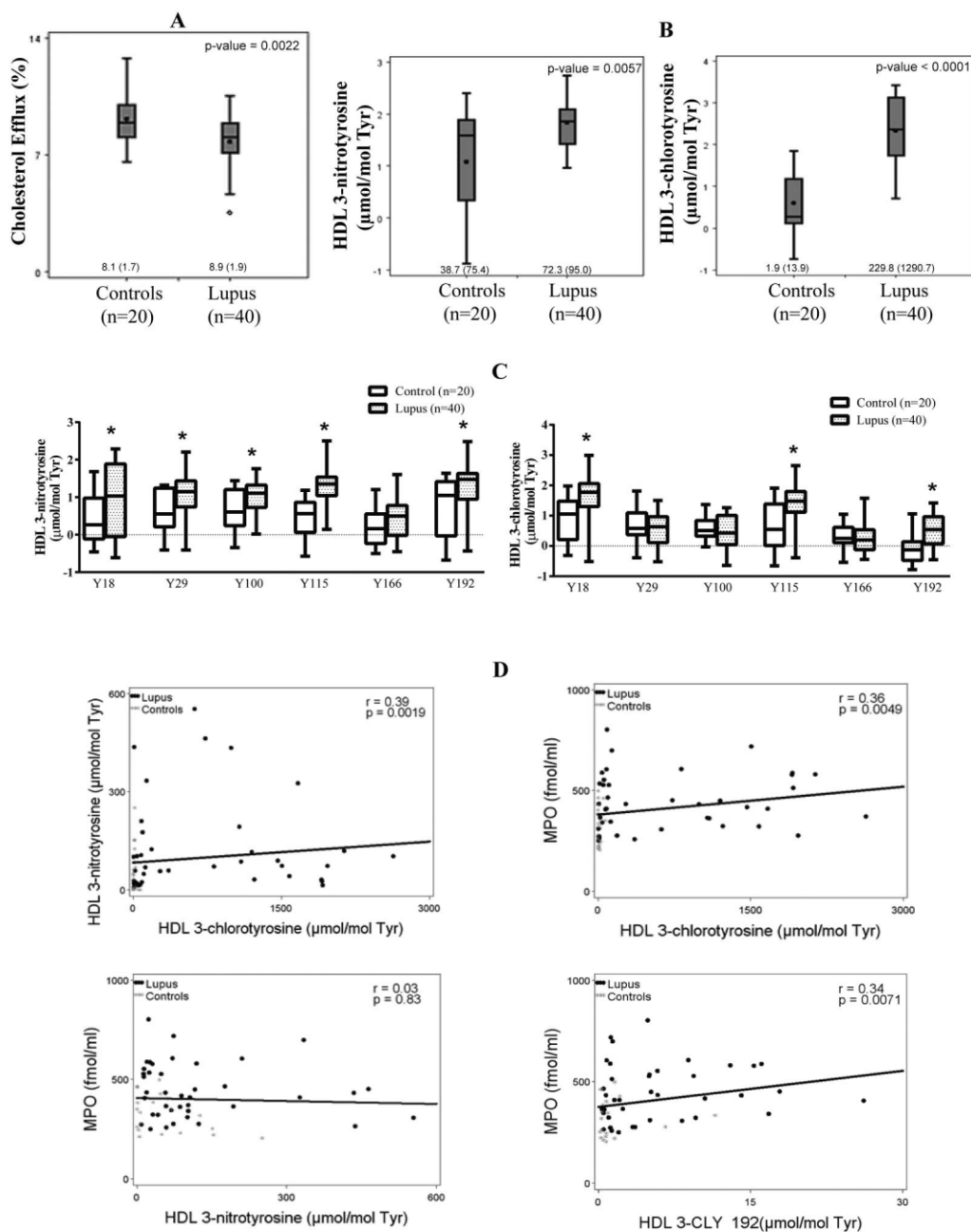


Figure 1. High-density lipoprotein (HDL) isolated from patients with systemic lupus erythematosus (SLE) is significantly oxidized and dysfunctional. Plasma and HDL from healthy controls and SLE patients were purified. **A**, ATP-binding cassette transporter A1-mediated cholesterol efflux capacity (determined in J774 cells loaded with radiolabeled ^3H -cholesterol and then incubated with SLE or control apolipoprotein B [Apo B]-depleted plasma) in controls and SLE patients. **B**, Reactive nitrogen species- and myeloperoxidase (MPO)-mediated 3-nitrotyrosine (N-Tyr) levels and MPO-specific 3-chlorotyrosine (Cl-Tyr) levels in HDL from controls and SLE patients. **C**, Distribution of isotopically labeled nitrated or chlorinated tyrosines. Native Apo A-I peptides were spiked into HDL samples from controls and SLE patients. Extracted ion chromatograms from specific fragment ions were used for quantitative analysis. Data in **A–C** are shown as box plots. Each box represents the interquartile range (IQR). Lines inside the boxes represent the median. Whiskers represent the highest value within the upper fence and the lowest value within the lower fence. Circles indicate outliers (>1.5 times the IQR). Data in **B** and **C** are displayed on the \log_{10} scale. Medians (IQR) are reported on the raw scale. * = $P < 0.05$ versus controls. **D**, Scatter plots and least squares regression lines showing correlations between levels of HDL N-Tyr and HDL Cl-Tyr oxidation, MPO and HDL Cl-Tyr oxidation, MPO and HDL N-Tyr oxidation, and MPO and chlorination levels at Tyr¹⁹² (HDL 3-CLY 192) within Apo A-I from SLE patients.

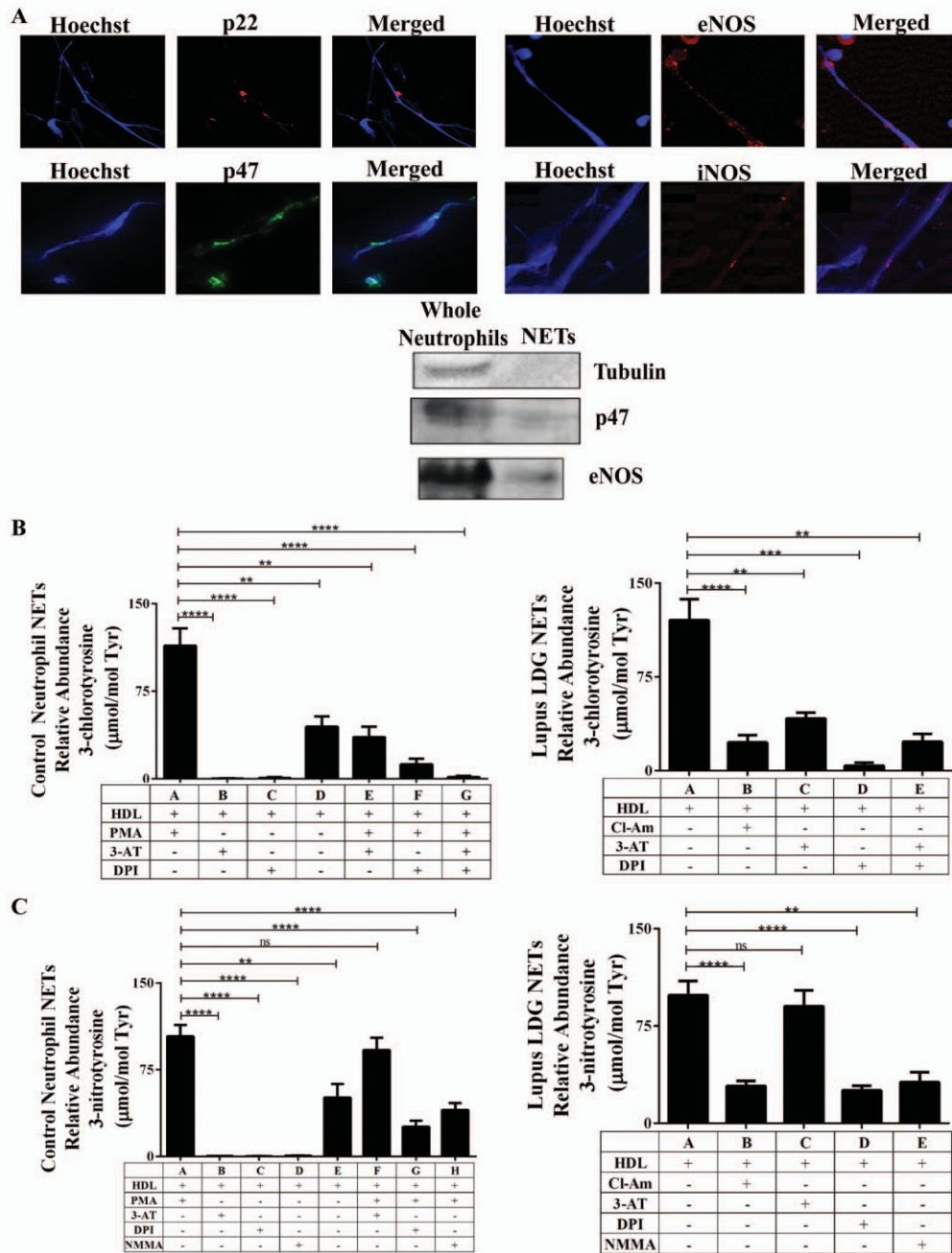


Figure 2. Neutrophil extracellular trap (NET)-derived myeloperoxidase (MPO), nitric oxide synthase (NOS), and NADPH oxidase (NOX) modify human high-density lipoprotein (HDL). Immunofluorescence staining and immunoblotting were used to identify possible enzymatic sources of HDL nitration. **A**, Detection of NOX subunits, p22 and p47, and 2 NOS isoforms, endothelial cell NOS (eNOS) and inducible NOS (iNOS), in human NETs. Control neutrophil NETs and lupus low-density granulocyte (LDG) NETs were added to control, nonoxidized HDL. Original magnification $\times 63$. **B** and **C**, Resulting levels of MPO-specific 3-chlorotyrosine (**B**), and reactive nitrogen species-mediated 3-nitrotyrosine (**C**) oxidation, as quantified by mass spectrometry. L-N^G-monomethyl-L-arginine (L-NMMA), diphenyleneiodonium (DPI), and 3-amino-1,2,4-triazole (3-AT) were added to block NOS, NOX, and MPO activity, respectively. The peptidylarginine deiminase inhibitor Cl-amidine (Cl-Am) was added to LDGs to block spontaneous NETosis. For control neutrophils, the absence of phorbol myristate acetate (PMA) stimulation was used as a negative control for NETosis. Bars show the mean \pm SEM ($n = 6$ subjects per group). $** = P < 0.007$; $*** = P = 0.0002$; $**** = P < 0.0001$. NS = not significant.

115, 100, 29, and 18 in SLE (Figure 1C). Taken together, these data suggest that regiospecific modifications to HDL by MPO and RNS, specifically at Tyr¹⁸, Tyr¹¹⁵, and Tyr¹⁹², may be of particular interest in the context of SLE-associated CVD.

When we examined correlations between levels of N-Tyr and Cl-Tyr in SLE HDL, they positively correlated with each other (Figure 1D) ($r = 0.39$, $P = 0.0019$), suggesting that these oxidative modifications are generated at similar sites. While levels of Cl-Tyr significantly correlated with plasma MPO levels (Figure 1D) ($r = 0.36$, $P = 0.0049$), there was no significant correlation between N-Tyr and MPO levels (Figure 1D) ($r = 0.03$, $P = 0.83$). This suggests that the RNS leading to HDL nitration are not primarily derived from MPO, but from another oxidative source. While tyrosines 115 and 18 displayed the highest levels of oxidation in lupus, Cl-Tyr 192 showed the most significant positive correlation with plasma MPO levels (Figure 1D). Overall, these results support the notion that in SLE, RNS- and MPO-derived oxidants modify HDL, thereby impairing lipoprotein function.

Oxidation in total plasma proteins was also determined (Table 2). Similar trends were observed as for HDL. Median plasma N-Tyr levels were 8.8-fold higher in lupus patients than in controls (286.0 versus 32.5 $\mu\text{moles/mole Tyr}$; $P < 0.0001$) and median plasma Cl-Tyr levels were 40.6-fold higher in lupus patients than in controls (33.3 versus 0.82 $\mu\text{moles/mole Tyr}$; $P < 0.0001$), which persisted after adjustment (Table 2; values in table are natural log transformed). As expected, the levels of plasma and HDL Cl-Tyr in SLE trended toward a negative correlation with CEC percentage, while HDL N-Tyr levels showed no significant association (data not shown) (14). Overall, this profile of enhanced HDL and total plasma protein oxidation is consistent with an environment of increased oxidative stress and impaired CEC in SLE.

Promotion of HDL oxidation in vitro by NET-derived MPO, NOX, and NOS. Since levels of RNS- and MPO-derived oxidative modifications are markedly elevated in lupus and correlate with functional impairment of CEC, we attempted to identify the putative sources of enhanced RNS and MPO activity in SLE. MPO HDL oxidation is classically attributed to plaque macrophages (12,24). Another possible source is peripheral blood MPO, which has been reported to be enhanced in SLE (21) and which we were able to confirm (Tables 1 and 2). Since a subset of neutrophils in the peripheral blood of lupus patients (LDGs) has a significantly enhanced capacity to form NETs, a source of externalized NOX and MPO, we examined if the NETs could induce HDL

oxidation (4,27,33). Additionally, because we found that MPO levels did not correlate with N-Tyr HDL levels (Figure 1D), we examined if an alternative producer of RNS (NOS and NOX formation of ONOO⁻) could be present in NETs and serve as a source of HDL nitration.

MPO (not shown), NOX, and NOS were all detected on both control and LDG NETs by fluorescence microscopy and immunoblotting (Figure 2A). Next, we exposed native HDL to NETs isolated from PMA-stimulated control neutrophils or spontaneously by lupus LDGs, in the absence or presence of MPO, NOX, and NOS inhibitors (3-AT, DPI, and L-NMMA, respectively) and examined the HDL oxidation profile. As shown in Figures 2B and C, NETs from both lupus LDGs and control neutrophils significantly enhanced HDL oxidation. HOCl, which is synthesized by MPO downstream of NOX activity, is the major source of HDL chlorination in humans. When netting control neutrophils and lupus LDGs were treated with 3-AT and DPI to block MPO and NOX activity, respectively, HDL Cl-Tyr oxidation was abrogated (Figure 2B). These results support the hypothesis that MPO and NOX externalized on NETs can induce Cl-Tyr HDL oxidation in the periphery.

Because both NOS and MPO are capable of producing the RNS required for HDL nitration, we used a KRPG solution with no added nitrite to examine the role of NOS alone in N-Tyr oxidation. Under these conditions, only NOS could generate the NO^{*} required for ONOO⁻ formation that could lead to HDL nitration. MPO, under these conditions, could not be the source of RNS. Indeed, the MPO inhibitor 3-AT was ineffective at blocking HDL nitration, while the NOS inhibitor L-NMMA significantly abrogated HDL N-Tyr oxidation for both LDGs and control neutrophils (Figure 2C). These results suggest that NET-bound NOS is a source of the RNS causing HDL nitration, and may explain why the levels of MPO did not correlate with the levels of N-Tyr-oxidized HDL in SLE.

Blockade of NET formation in vitro by CQ. We determined the effect of physiologically relevant concentrations of CQ (250 ng/ml) on NET formation (17). CQ significantly inhibited NET formation in control neutrophils and lupus LDGs (Figures 3A–C). To assess if CQ modified MPO, NOS, and NOX activity, neutrophils were homogenized, treated with CQ, and incubated with HDL. CQ did not significantly block HDL Cl-Tyr or N-Tyr oxidation in lupus LDGs or control neutrophils (data not shown). Therefore, the inhibitory effects of CQ on NET formation do not occur by inhibition of oxidative enzyme activity.

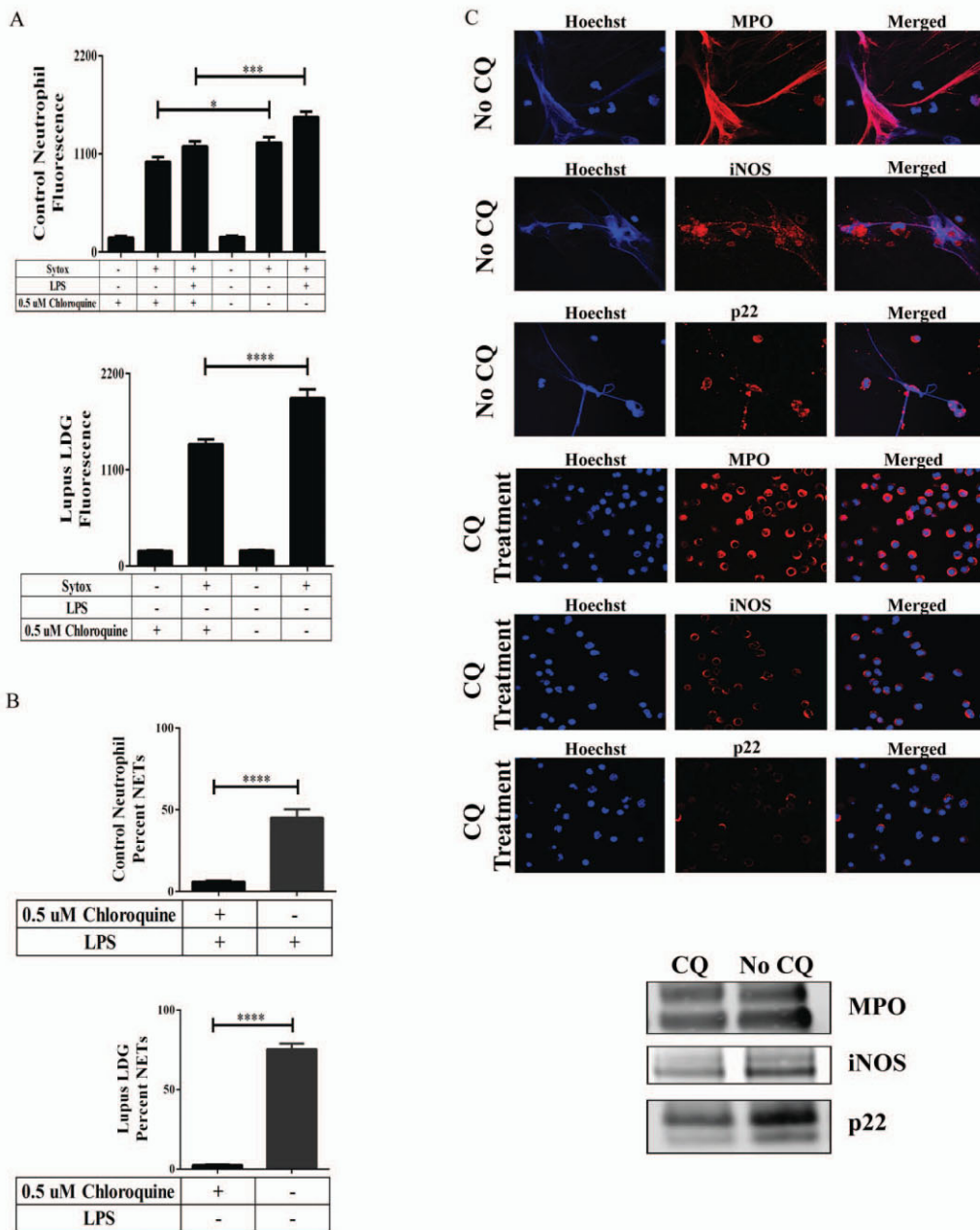


Figure 3. Chloroquine (CQ) abrogates NET formation. **A**, Control neutrophil and lupus LDG fluorescence. Control neutrophils or lupus LDGs were purified from whole blood, treated with or without CQ, and assessed for DNA externalization via Sytox assay. **B** and **C**, Quantification of NET production (**B**) and MPO, iNOS, and p22 externalization on the NETs (**C**), determined by immunofluorescence staining of cells treated with or without CQ. Original magnification $\times 63$ in **C**. Bars in **A** and **B** show the mean \pm SEM ($n = 5$ subjects per group). $* = P = 0.01$; $*** = P = 0.0001$; $**** = P < 0.0001$. LPS = lipopolysaccharide (see Figure 2 for other definitions).

NET-derived NOS and NOX are sources of HDL oxidation in murine systems. While present in murine NETs, MPO is not associated with murine atherosclerosis (24,47). Lupus-prone NZM mice display striking

elevations of N-Tyr HDL oxidation, but not Cl-Tyr HDL oxidation, when compared to control mice (5), possibly because murine leukocytes contain less MPO, the sole known source of Cl-Tyr oxidation, than human leuko-

cytes (12,24,47). We therefore examined if NOX and NOS were present in murine NETs and could produce RNS to form N-Tyr-oxidized HDL (26,33). We identified NOS and NOX machinery present in PMA-induced murine NETs (Figure 4A). To verify that these NET-bound enzymes could cause HDL oxidation, we exposed native HDL from non-lupus-prone BALB/c mice to proteins purified from digested NETs from NZM or BALB/c mice in the absence or presence of MPO, NOX, and NOS inhibitors (3-AT, DPI, and L-NMMA, respectively) and examined HDL oxidation profiles (26,27,32,33,44,45). Consistent with our previous observations, we found no significant Cl-Tyr-oxidized HDL patterns after HDL incubation with murine NETs (Figure 4B) (5). However, a significant oxidation pattern for N-Tyr-oxidized HDL was observed (Figure 4C). While experiments were performed in nitrite-containing media so that either NOS or MPO could potentially promote HDL nitration, only DPI and L-NMMA significantly blocked NET-induced N-Tyr HDL oxidation. These results support the idea that MPO is less active in mice and that NOX and NOS are the primary sources of the oxidative species required for HDL nitration in murine systems.

Finally, to verify that NETs are an important source of HDL oxidation in the periphery, we inhibited NET formation in NZM mice *in vivo* and examined their oxidative profile. NZM mice received the PAD inhibitor Cl-amidine daily for 14 weeks, since PAD activity is necessary for NET formation (6,34). Cl-amidine-treated mice displayed significantly decreased N-Tyr content in HDL, but not total plasma, when compared to vehicle-treated mice (Figure 4D). These results indicate that *in vivo* inhibition of NET formation in lupus-prone mice decreases HDL oxidation.

DISCUSSION

Part of the high risk of CVD observed in SLE may be related to increased levels and activity of oxidative enzymes that transform HDL into a dysfunctional proatherogenic lipoprotein (1,3,21). We found that lupus plasma exhibited impaired CEC, and SLE patients had significantly increased plasma MPO levels and highly Cl-Tyr- and N-Tyr-oxidized plasma proteins, including HDL Apo A-I. HDL nitration did not correlate with MPO levels, indicating an alternate source of RNS. However, Cl-Tyr- and N-Tyr-oxidized HDL levels correlated with each other, suggesting that both modifications occur at similar sites in the vasculature, though not through the same enzyme. Because of the link

between SLE and enhanced NET formation, we hypothesized that the enzymatic sources of the proatherogenic oxidized HDL were derived from active NOS, MPO, and NOX present in NETs. Indeed, previous studies suggest that these oxidative enzymes may have enhanced activity while bound on NETs (26). All 3 oxidative enzymes were detected and functional in NETs, as demonstrated when mass spectrometric analysis performed on HDL incubated with NETs revealed oxidative modifications (chlorination and nitration). Use of specific inhibitors for each of these enzymes reduced this oxidation, further confirming functional activity of these NET enzymes. Finally, we demonstrated that pharmacologic *in vivo* NET inhibition potently decreased levels of proinflammatory N-Tyr-oxidized HDL in lupus-prone mice. These observations suggest a crucial role for NETs in the transformation of HDL into its proinflammatory form.

The connection between NET oxidation of HDL and plasma proteins is particularly interesting and novel in the context of chronic inflammatory conditions such as SLE, RA, and vasculitis (8,28). Since lupus patients exhibit both accelerated NET formation and impaired NET degradation, these structures represent a potent and long-term source of externalized oxidative material (4,29,30). Most of the literature to date has focused on atherosclerotic plaque macrophages as sources of MPO-driven HDL oxidation, yet circulating neutrophils contain higher levels of MPO than tissue-resident macrophages (12,24), and neutrophils and NETs are present around thrombotic and atheroma plaques (35,38,39,48). The high concentration of MPO in NETs may even specifically attract HDL for oxidation. Consistent with previous reports, we found that Cl-Tyr levels in HDL are higher than in circulating plasma proteins, suggesting specific targeting of HDL (8,18). While other investigators have demonstrated that neutrophils can cause protein oxidation, our observations are the first to specifically implicate active MPO, NOX, and NOS in NETs as sources of HDL oxidation (44), and to demonstrate NOS in NETs. Which NOS isoform is required for NET-derived HDL oxidation is not yet clear. Nonetheless, NOS activity in NETs and its association with HDL nitration opens potential avenues for CVD therapies.

To our knowledge, this is the first study to show that physiologic concentrations of antimalarials significantly inhibit NET formation *in vitro*. Previous evidence suggested that antimalarials are effective in SLE through modulation of Toll-like receptors and antigen presentation (49,50). We now describe an additional putative protective role of antimalarials in autoimmunity through modulation of NET formation. While use of antimalar-

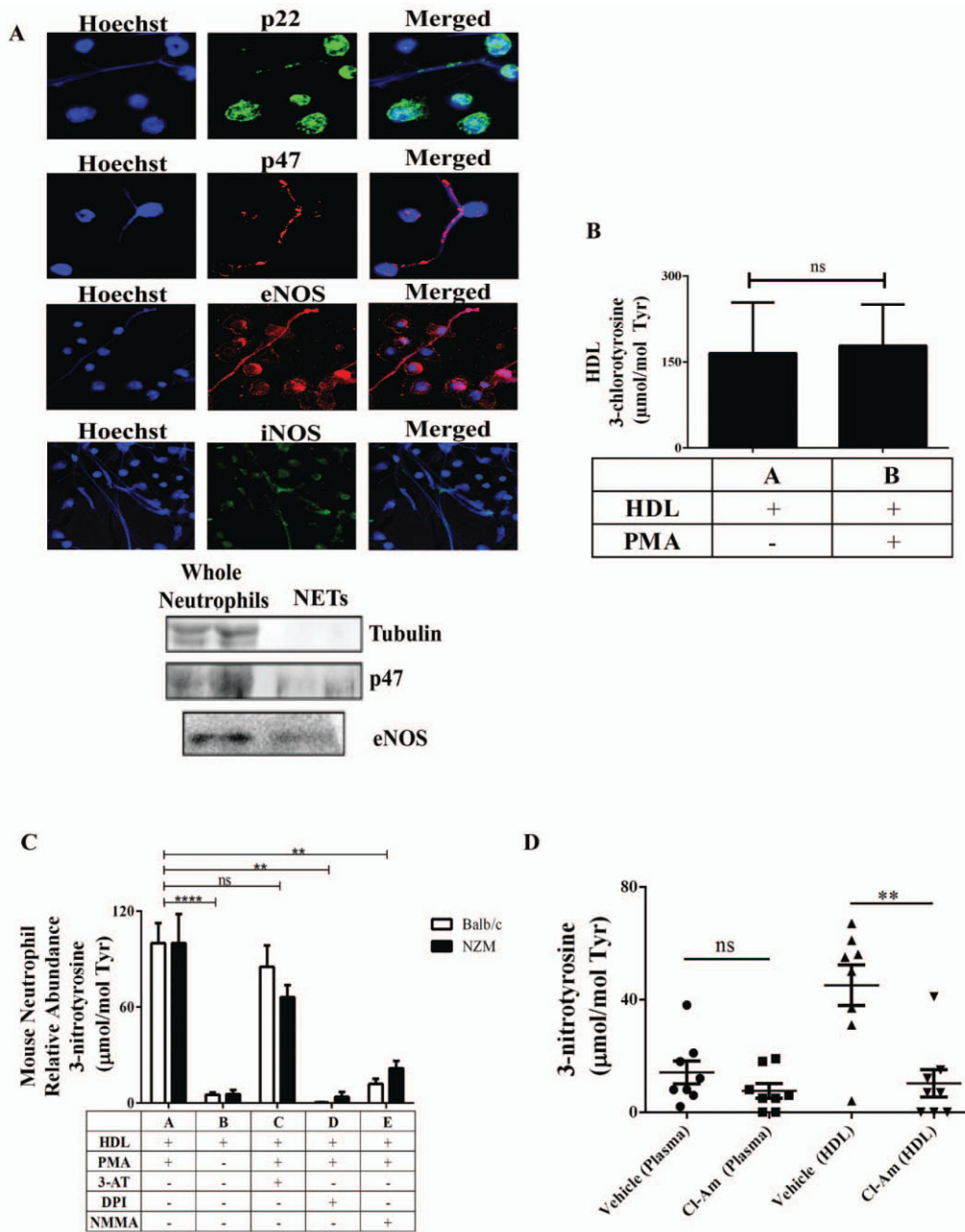


Figure 4. NET-derived NOS and NOX induce HDL oxidation in mice, while NET inhibition decreases HDL oxidation in vivo. Immunofluorescence staining and immunoblotting were used to identify possible enzymatic sources of HDL nitration. **A**, Detection of NOX subunits, p22 and p47, and 2 NOS isoforms, eNOS and iNOS, in murine NETs. NETs from control BALB/c mice and NZM2328 (NZM) mice with lupus were added to control, nonoxidized murine HDL. Original magnification $\times 63$. **B**, Resulting levels of MPO-specific 3-chlorotyrosine oxidation in the absence or presence of isolated NETs, as quantified by mass spectrometry. Bars show the mean \pm SEM ($n = 4$ mice per group). **C**, Resulting levels of NOS- and NOX-mediated 3-nitrotyrosine oxidation, as quantified by mass spectrometry. L-NMMA, DPI, and 3-AT were added to block NOS, NOX, and MPO activity, respectively. The absence of PMA stimulation was used as a negative control for NET formation. Comparisons were made within the same mouse strain. Bars show the mean \pm SEM ($n = 8$ mice per group). **D**, Levels of plasma and HDL 3-nitrotyrosine content in 26-week-old NZM mice that had received daily injections of phosphate buffered saline (vehicle; $n = 8$) or Cl-amide ($n = 8$) for 14 weeks. Symbols represent individual mice; horizontal lines and error bars show the median and SEM. ** = $P < 0.01$; **** = $P < 0.0001$. See Figure 2 for other definitions.

ials associated only with plasma N-Tyr oxidation, the small sample size might have limited observing an effect. This should be further explored in future studies.

The current study has some limitations. The effects on CEC reduction of 15% might appear modest, but we previously reported similar results in RA (8). Recent clinical studies have demonstrated smaller, though statistically significant, percent reductions in CEC with larger CVD and psoriasis cohort sample sizes (17,43). Our results therefore are consistent with the findings of these studies and even show a greater reduction in CEC than in traditional CVD. Further, while we focused on total HDL in this study, HDL subpopulations might be different in lupus patients compared to control subjects and might account for altered susceptibility.

The proatherogenic effects of NETs include direct vascular cytotoxicity, activation of macrophage inflammasomes, and induction of procoagulant pathways (1,28–31,37,48). Overall, this study suggests an additional proatherogenic mechanism by which NET-derived MPO/NOX- and NOS/NOX-generated oxidative species may generate dysfunctional HDL in SLE. HDL oxidation in SLE may take place in the periphery rather than the vascular wall (1,31). Given its small particle size and active circulation during cholesterol efflux, HDL is, conceivably, more readily trapped by NETs in the blood vessel lumen, endothelium, or sites of inflammation, rather than in subendothelial atherosclerotic lesions (17,35,36). NET-mediated modification of HDL may lead to a dysfunctional lipoprotein, impairing CEC and promoting proinflammatory responses in blood vessels and the periphery.

AUTHOR CONTRIBUTIONS

All authors were involved in drafting the article or revising it critically for important intellectual content, and all authors approved the final version to be published. Drs. Pennathur and Kaplan had full access to all of the data in the study and take responsibility for the integrity of the data and the accuracy of the data analysis.

Study conception and design. Smith, Vivekanandan-Giri, Carmona-Rivera, Subramanian, Pennathur, Kaplan.

Acquisition of data. Smith, Vivekanandan-Giri, Tang, Knight, Mathew, Carmona-Rivera, Liu, Subramanian, Hasni, Thompson, Heinecke, Saran, Pennathur.

Analysis and interpretation of data. Smith, Vivekanandan-Giri, Knight, Mathew, Padilla, Gillespie, Carmona-Rivera, Subramanian, Heinecke, Saran, Pennathur, Kaplan.

REFERENCES

1. Kahlenberg JM, Kaplan MJ. Mechanisms of premature atherosclerosis in rheumatoid arthritis and lupus. *Annu Rev Med* 2013;64:249–63.
2. Esdaile JM, Abrahamowicz M, Grodzicky T, Li Y, Panaritis C, du Berger R, et al. Traditional Framingham risk factors fail to fully account for accelerated atherosclerosis in systemic lupus erythematosus. *Arthritis Rheum* 2001;44:2331–7.
3. Ronda N, Favari E, Borghi MO, Ingegnoli F, Gerosa M, Chighizola C, et al. Impaired serum cholesterol efflux capacity in rheumatoid arthritis and systemic lupus erythematosus. *Ann Rheum Dis* 2014;73:609–15.
4. Villanueva E, Yalavarthi S, Berthier CC, Hodgins JB, Khandpur R, Lin AM, et al. Netting neutrophils induce endothelial damage, infiltrate tissues, and expose immunostimulatory molecules in systemic lupus erythematosus. *J Immunol* 2011;187:538–52.
5. Thacker SG, Zhao W, Smith CK, Luo W, Wang H, Vivekanandan-Giri A, et al. Type I interferons modulate vascular function, repair, thrombosis, and plaque progression in murine models of lupus and atherosclerosis. *Arthritis Rheum* 2012;64:2975–85.
6. Knight JS, Zhao W, Luo W, Subramanian V, O'Dell AA, Yalavarthi S, et al. Peptidylarginine deiminase inhibition is immunomodulatory and vasculoprotective in murine lupus. *J Clin Invest* 2013;123:2981–93.
7. Denny MF, Yalavarthi S, Zhao W, Thacker SG, Anderson M, Sandy AR, et al. A distinct subset of proinflammatory neutrophils isolated from patients with systemic lupus erythematosus induces vascular damage and synthesizes type I IFNs. *J Immunol* 2010;184:3284–97.
8. Vivekanandan-Giri A, Slocum JL, Byun J, Tang C, Sands RL, Gillespie BW, et al. High density lipoprotein is targeted for oxidation by myeloperoxidase in rheumatoid arthritis. *Ann Rheum Dis* 2013;72:1725–31.
9. McMahon M, Grossman J, Skaggs B, FitzGerald J, Sahakian L, Ragavendra N, et al. Dysfunctional proinflammatory high-density lipoproteins confer increased risk of atherosclerosis in women with systemic lupus erythematosus. *Arthritis Rheum* 2009;60:2428–37.
10. Ansell BJ, Fonarow GC, Fogelman AM. The paradox of dysfunctional high-density lipoprotein. *Curr Opin Lipidol* 2007;18:427–34.
11. Zhang R, Brennan ML, Fu X, Aviles RJ, Pearce GL, Penn MS, et al. Association between myeloperoxidase levels and risk of coronary artery disease. *JAMA* 2001;286:2136–42.
12. Karakas M, Koenig W. Myeloperoxidase production by macrophage and risk of atherosclerosis. *Curr Atheroscler Rep* 2012;14:277–83.
13. Shao B, Pennathur S, Heinecke JW. Myeloperoxidase targets apolipoprotein A-I, the major high density lipoprotein protein, for site-specific oxidation in human atherosclerotic lesions. *J Biol Chem* 2012;287:6375–86.
14. Shao B, Bergt C, Fu X, Green P, Voss JC, Oda MN, et al. Tyrosine 192 in apolipoprotein A-I is the major site of nitration and chlorination by myeloperoxidase, but only chlorination markedly impairs ABCA1-dependent cholesterol transport. *J Biol Chem* 2005;280:5983–93.
15. Assinger A, Koller F, Schmid W, Zellner M, Babeluk R, Koller E, et al. Specific binding of hypochlorite-oxidized HDL to platelet CD36 triggers proinflammatory and procoagulant effects. *Atherosclerosis* 2010;212:153–60.
16. Suzuki M, Pritchard DK, Becker L, Hoofnagle AN, Tanimura N, Bammler TK, et al. High-density lipoprotein suppresses the type I interferon response, a family of potent antiviral immunoregulators, in macrophages challenged with lipopolysaccharide. *Circulation* 2010;122:1919–27.
17. Furst DE. Pharmacokinetics of hydroxychloroquine and chloroquine during treatment of rheumatic diseases. *Lupus* 1996;Suppl 1:S11–5.
18. Pennathur S, Bergt C, Shao B, Byun J, Kassim SY, Singh P, et al. Human atherosclerotic intima and blood of patients with established coronary artery disease contain high density lipoprotein damaged by reactive nitrogen species. *J Biol Chem* 2004;279:42977–83.

19. Griendling KK. Novel NAD_pH oxidases in the cardiovascular system. *Heart* 2004;90:491–3.
20. Kubala L, Lu G, Baldus S, Berglund L, Eiserich JP. Plasma levels of myeloperoxidase are not elevated in patients with stable coronary artery disease. *Clin Chim Acta* 2008;394:59–62.
21. Telles RW, Ferreira GA, da Silva NP, Sato EI. Increased plasma myeloperoxidase levels in systemic lupus erythematosus. *Rheumatol Int* 2010;30:779–84.
22. Tsutsui M, Shimokawa H, Otsuji Y, Yanagihara N. Pathophysiological relevance of NO signaling in the cardiovascular system: novel insight from mice lacking all NO synthases. *Pharmacol Ther* 2010;128:499–508.
23. Bolli R. Cardioprotective function of inducible nitric oxide synthase and role of nitric oxide in myocardial ischemia and preconditioning: an overview of a decade of research. *J Mol Cell Cardiol* 2001;33:1897–918.
24. McMillen TS, Heinecke JW, LeBoeuf RC. Expression of human myeloperoxidase by macrophages promotes atherosclerosis in mice. *Circulation* 2005;111:2798–804.
25. Cedergren J, Follin P, Forslund T, Lindmark M, Sundqvist T, Skogh T. Inducible nitric oxide synthase (NOS II) is constitutive in human neutrophils. *APMIS* 2003;111:963–8.
26. Munafò DB, Johnson JL, Brzezinska AA, Ellis BA, Wood MR, Catz SD. DNase I inhibits a late phase of reactive oxygen species production in neutrophils. *J Innate Immun* 2009;1:527–42.
27. Fuchs TA, Abed U, Goosmann C, Hurwitz R, Schulze I, Wahn V, et al. Novel cell death program leads to neutrophil extracellular traps. *J Cell Biol* 2007;176:231–41.
28. Khandpur R, Carmona-Rivera C, Vivekanandan-Giri A, Gizinski A, Yalavarthi S, Knight JS, et al. NETs are a source of citrullinated autoantigens and stimulate inflammatory responses in rheumatoid arthritis. *Sci Transl Med* 2013;5:178ra40.
29. Leffler J, Martin M, Gullstrand B, Tyden H, Lood C, Truedsson L, et al. Neutrophil extracellular traps that are not degraded in systemic lupus erythematosus activate complement exacerbating the disease. *J Immunol* 2012;188:3522–31.
30. Hakkim R, Furnrohr BG, Amann K, Laube B, Abed UA, Brinkmann V, et al. Impairment of neutrophil extracellular trap degradation is associated with lupus nephritis. *Proc Natl Acad Sci U S A* 2010;107:9813–8.
31. Kahlenberg JM, Carmona-Rivera C, Smith CK, Kaplan MJ. Neutrophil extracellular trap-associated protein activation of the NLRP3 inflammasome is enhanced in lupus macrophages. *J Immunol* 2013;190:1217–26.
32. Metzler KD, Fuchs TA, Nauseef WM, Reumaux D, Roesler J, Schulze I, et al. Myeloperoxidase is required for neutrophil extracellular trap formation: implications for innate immunity. *Blood* 2011;117:953–9.
33. Kirchner T, Moller S, Klinger M, Solbach W, Laskay T, Behnen M. The impact of various reactive oxygen species on the formation of neutrophil extracellular traps. *Mediators Inflamm* 2012;2012:849136.
34. Leshner M, Wang S, Lewis C, Zheng H, Chen XA, Santy L, et al. PAD4 mediated histone hypercitrullination induces heterochromatin decondensation and chromatin unfolding to form neutrophil extracellular trap-like structures. *Front Immunol* 2012;3:307.
35. Megens RT, Vijayan S, Lievens D, Doring Y, van Zandvoort MA, Grommes J, et al. Presence of luminal neutrophil extracellular traps in atherosclerosis. *Thromb Haemost* 2012;107:597–8.
36. Fuchs TA, Brill A, Wagner DD. Neutrophil extracellular trap (NET) impact on deep vein thrombosis. *Arterioscler Thromb Vasc Biol* 2012;32:1777–83.
37. Doring Y, Manthey HD, Drechsler M, Lievens D, Megens RT, Soehnlein O, et al. Auto-antigenic protein-DNA complexes stimulate plasmacytoid dendritic cells to promote atherosclerosis. *Circulation* 2012;125:1673–83.
38. Soehnlein O. Multiple roles for neutrophils in atherosclerosis. *Circ Res* 2012;110:875–88.
39. Dorweiler B, Torzewski M, Dahm M, Kirkpatrick CJ, Lackner KJ, Vahl CF. Subendothelial infiltration of neutrophil granulocytes and liberation of matrix-destabilizing enzymes in an experimental model of human neo-intima. *Thromb Haemost* 2008;99:373–81.
40. Hochberg MC, for the Diagnostic and Therapeutic Criteria Committee of the American College of Rheumatology. Updating the American College of Rheumatology revised criteria for the classification of systemic lupus erythematosus [letter]. *Arthritis Rheum* 1997;40:1725.
41. Isenberg D, Bacon P, Bombardier C, Gladman D, Goldsmith CH, Kalunian K, et al. Criteria for assessing disease activity in systemic lupus erythematosus. *J Rheumatol* 1989;16:1395–6.
42. Vivekanandan-Giri A, Byun J, Pennathur S. Quantitative analysis of amino acid oxidation markers by tandem mass spectrometry. *Methods Enzymol* 2011;491:73–89.
43. Khera AV, Cuchel M, de la Llera-Moya M, Rodrigues A, Burke MF, Jafri K, et al. Cholesterol efflux capacity, high-density lipoprotein function, and atherosclerosis. *N Engl J Med* 2011;364:127–35.
44. Bergt C, Marsche G, Panzenboeck U, Heinecke JW, Malle E, Sattler W. Human neutrophils employ the myeloperoxidase/hydrogen peroxide/chloride system to oxidatively damage apolipoprotein A-I. *Eur J Biochem* 2001;268:3523–31.
45. Goud AP, Goud PT, Diamond MP, Gonik B, Abu-Soud HM. Activation of the cGMP signaling pathway is essential in delaying oocyte aging in diabetes mellitus. *Biochemistry* 2006;45:11366–78.
46. Causey CP, Jones JE, Slack JL, Kamei D, Jones LE, Subramanian V, et al. The development of N- α -(2-carboxyl)benzoyl-N(5)-(2-fluoro-1-iminoethyl)-l-ornithine amide (o-F-amidine) and N- α -(2-carboxyl)benzoyl-N(5)-(2-chloro-1-iminoethyl)-l-ornithine amide (o-Cl-amidine) as second generation protein arginine deiminase (PAD) inhibitors. *J Med Chem* 2011;54:6919–35.
47. Brennan ML, Anderson MM, Shih DM, Qu XD, Wang X, Mehta AC, et al. Increased atherosclerosis in myeloperoxidase-deficient mice. *J Clin Invest* 2001;107:419–30.
48. Carmona-Rivera C, Zhao W, Yalavarthi S, Kaplan MJ. Neutrophil extracellular traps induce endothelial dysfunction in systemic lupus erythematosus through the activation of matrix metalloproteinase-2. *Ann Rheum Dis* 2014. E-pub ahead of print.
49. Fox R. Anti-malarial drugs: possible mechanisms of action in autoimmune disease and prospects for drug development. *Lupus* 1996;5 Suppl 1:S4–10.
50. Kuznik A, Bencina M, Svajger U, Jeras M, Rozman B, Jerala R. Mechanism of endosomal TLR inhibition by antimalarial drugs and imidazoquinolines. *J Immunol* 2011;186:4794–804.